applied sciences

MDPI

Article

Improvement of Electro-Optical Properties of PSLC Devices by Silver Nanowire Doping

Xudong Yan [1,2], Wei Liu [1,2], Yong Zhou [1,2], Dong Yuan [1,2,*], Xiaowen Hu [1,2], Wei Zhao [1,2,3] and Guofu Zhou [1,2,3,*]

1 Guangdong Provincial Key Laboratory of Optical Information Materials and Technology & Institute of Electronic Paper Displays, South China Academy of Advanced Optoelectronics, South China Normal University, Guangzhou 510006, China; yan-xudong@m.scnu.edu.cn (X.Y.); liu-wei@m.scnu.edu.cn (W.L.); zhou-yong@m.scnu.edu.cn (Y.Z.); xwhu@m.scnu.edu.cn (X.H.); 20181010@m.scnu.edu.cn (W.Z.)

2 SCNU-TUE Joint Lab of Device Integrated Responsive Materials (DIRM), National Center for International Research on Green Optoelectronics, South China Normal University, No 378, West Waihuan Road, Guangzhou Higher Education Mega Center, Guangzhou 510006, China.

3 Shenzhen Guohua Optoelectronics Tech. Co. Ltd., Shenzhen 518110, China

* Correspondence: yuandong@scnu.edu.cn (D.Y.); guofu.zhou@m.scnu.edu.cn (G.Z.); Tel.: +86-136-314-99077 (D.Y.)

Received: 29 November 2018; Accepted: 24 December 2018; Published: 3 January 2019

Featured Application: The PSLC device studied in this work could be used as privacy windows and provide a convenient indoor environment. Doping of silver nanowires optimizes the performance of PSLC smart windows.

Abstract: Polymer stabilized liquid crystal (PSLC) devices modulating the light that goes through them have broad applications. In this study, to improve the electro-optical properties of a PSLC device, Ag nanowires with diameter about 20 nm were doped into PSLC active layer with different concentrations. The influence of Ag nanowires concentration on the driving voltage, on-state response time and frequency modulation characteristics of a PSLC device were studied. The results indicate that the doping of Ag nanowires can reduce the driving voltage of PSLC cell up to 42%. The response time of the PSLC cell can decrease by about 41%. Meanwhile, frequency modulation does not show significant improvement upon Ag nanowire doping. Overall, Ag nanowire doping can improve the electro-optical properties of PSLC device effectively.

Keywords: PSLC device; Silver nanowires doping; Electro-optical property; Smart glass; Privacy window

1. Introduction

Smart windows [1,2] that can modulate light are a type of intelligent building material and can save energy in buildings. At present, most commercially available smart windows are controlled by electric field. Materials with such function are mainly liquid crystal (LC) [3–5] and electrochromic oxide. For LC based smart windows, the orientation of LC molecule will change when an electronic field is applied. The incident light will be modulated by the LC molecules, and be reflected, scattered and so on. Electrochromic materials show a change of color as induced either by an electron transfer (redox) process or by a sufficiently high electrochemical potential [6]. Compared with electrochromic smart glass, LC based smart glass has many advantages, such as low cost, good stability, easy regulation and fabrication of large size preparation. As a result, LC based smart windows are expected to occupy the mainstream of smart glass market [7].

Privacy windows that can switch between scatting state and transparent state are one of the most popular types of LC-based smart glass. There are two kinds of privacy windows: polymer dispersed

liquid crystal (PDLC) based and polymer stabilized liquid crystal (PSLC) based [8–10]. PDLC is a composite material with submicron LC droplets embedded in a polymer matrix. Without an electric field, the LC molecules in the PDLC device are randomly orientated, scattering the incident light and the device is opaque. When an electric field is applied, the LC molecules are reoriented into the same direction and the device becomes transparent, with the transmittance approaching 90% with a sufficiently high electric field [11]. On the contrary, PSLC incorporates only small amount of polymer into LC material to stabilize the orientation of LC molecules. Without electric field, the LC molecules are orientated in the same direction as alignment layer and the polymer, and the device is transparent. With an applied electric field, the LC molecules are reoriented to the perpendicular direction. Since the polymer network will disturb and impede the rotation of LC molecules, a multi-domain structure will form and the incident light will be scattered, causing the device to become opaque [12]. In application, PSLC devices, which are transparent without electric field, are more economical and convenient than PDLC devices. Furthermore, PSLC devices have lower threshold voltage, shorter response time, higher contrast and wide viewing angle [13], making them also widely used as displays, spatial light modulators, hologram-formed light modulators [14], temperature sensors [15], flexible displays [16], and other devices besides smart windows.

Although PSLC devices have been widely used, the critical electro-optical performance of the devices still needs to be optimized, including threshold voltage, response time and other optical parameters. In recent years, nanoscale materials have been widely used to improve the electro-optical response properties of LCs [17–19]. It has been found that the dispersed nanomaterial can change the properties of the host LC, such as the electrical, optical and magnetic properties [20]. At the same time, the nanomaterial can trap ions in LC material, decreasing the ion concentration and conductivity of LC, which would improve the electro-optical property of the LC host [21]. Chou et al. doped titania nanoparticles of different sizes in nematic LCs. They observed that smaller size nanoparticles can lower the threshold voltage of the device [22]. Others have doped metal oxide nanoparticles (MgO, SiO_2 and Y_2O_3) [23,24] in a nematic LC matrix. The order parameters of the LC-NP composite are reduced, which leads to a reduction in the threshold voltage required to redirect the LC director along the applied electric field.

The doping of noble metal nanoparticles in PDLC device will cause surface plasmon excitation at the nanoparticle–polymer interface [25] and influence the electro-optical properties of PDLC. Yaroshchuk et al. used inorganic nanoparticles to improve the view angle of PDLC [26,27]. Zhang et al. found the droplet size in PDLC decreases with the increase of Ag nanoparticle concentration, thus reducing the response time [28]. Filpo et al. doped single-walled carbon nanotubes (SWNTs) in reverse PDLC. They found that the driving voltage was reduced [29]. Wang et al. doped nano-graphite in PDLC devices and reduced the driving voltage [30]. Hinojosa et al. reported the surface plasmon excitation of doped Au nanoparticles improves the transmittance and driving voltage of PDLC [31]. Choi et al. used a silver nanowire–graphene oxide hybrid electrode to prepare a flexible polymer dispersed liquid crystal display, which makes the electro-optical performance of PDLC superior [32]. Nanoparticles are also doped in polymer stabilized cholesteric liquid crystal (PSCLC) to improve device performance. Zhang et al. doped Fe_xNi_y nanoparticles into the PSCLC film, which extends the viewing angle of PSCLC and improves the frequency response [33].

Inspired by these works, and to improve the electro-optical properties of PSLC devices, this study doped Ag nanowires in PSLC devices. The effects of Ag nanowires concentrations on the electro-optical properties of PSLC were studied, including driving voltage, response time and frequency modulation.

2. Materials and Methods

The working principle of PSLC device fabricated in this study is shown in Figure 1. When no electric field is applied, the negative LC and polymer molecules are orientated perpendicularly to the substrate. In this state, the incident light will not be scattered and the device is transparent. When an electric field is applied, the negative LC molecules want to orientate parallel to the substrate, but the

polymer network will disturb the rotation and a multi-domain structure will form. The incident light will be scattered and the device becomes opaque.

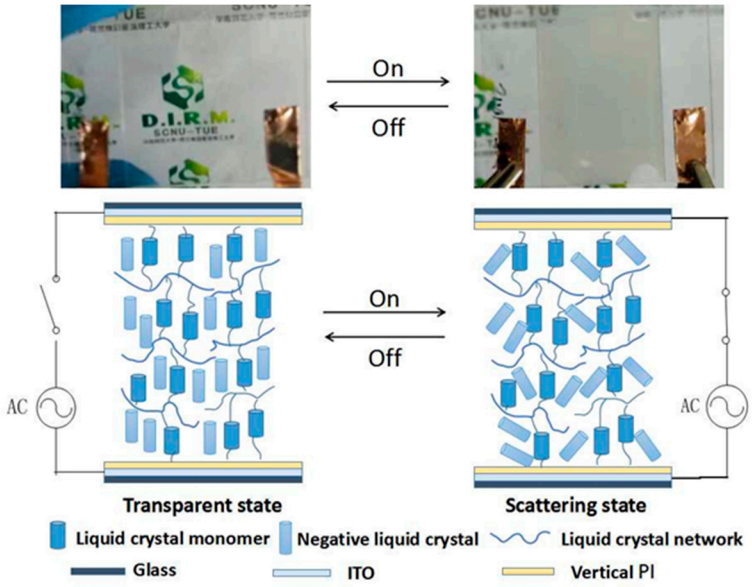

Figure 1. Schematic of PSLC device without electric field (transparent state) and with electric field (scattering state).

2.1. Materials

The silver nanowires used in this study (purchased from Shanghai Chaowei New Materials Co., Ltd., Shanghai, China) have diameter of 20–35 nm and a length of 10-20 μm. The SEM image of the silver nanowires is shown in Figure 2.

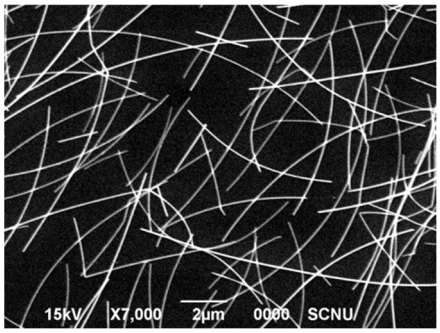

Figure 2. SEM image of Ag nanowires used in the experiment.

The materials used in the PSLC device include a negative LC mixture, a photo polymerizable LC monomer and a photo initiator. The negative LC mixture was purchased from Jiangsu Hecheng new materials Co. Ltd., Nanjing, China. The dielectric constant ΔE is −8.3, n_e is 1.633, n_o is 1.484, melting point is −40 °C, and clear point is 94 °C. The photo polymerizable monomer used in this study is RM82 from Merck KGaA, Darmstadt, Germany. The photo initiator is Irgacure 651 (IR651, BASF SE, Ludwigshafen, Germany). The liquid crystal monomer has acrylate groups at both ends. Under UV irradiation, these acrylate groups will react with each other and form a polymer network. This reaction was started by the photo-initiator. The molecular structure of RM82 and IR651 are shown in Figure 3. The alignment agent used in this study is a vertically oriented polyimide purchased from Shenzhen Dalton electronic materials Co. Ltd., Shenzhen, China.

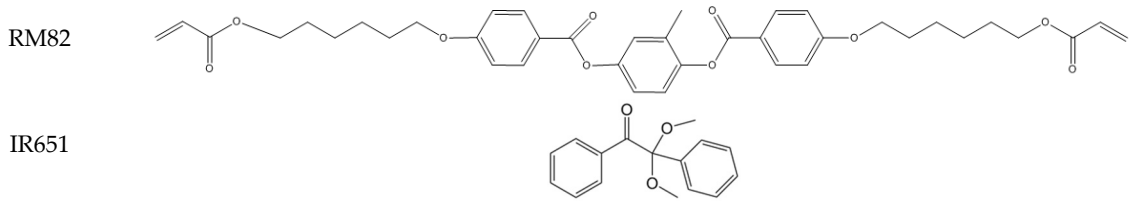

Figure 3. Materials used for PSLC compositions.

The concentration of materials used for PSLC fabrication in this study is shown in Table 1. The amount of negative LC was adjusted slightly when the concentration of silver nanowire changed.

Table 1. Proportion of materials required for the experiment.

Experimental Materials	Concentration
Negative LC	96.5 wt.%
RM82	3 wt.%
IR651	0.5 wt.%
Silver nanowires	0.01, 0.02, 0.05, 0.1 wt.%

2.2. Fabrication Process of PSLC Device

The PSLC mixture with negative LC, RM82 and IR651 were mixed together according to the ratio in Table 1 with magnetic stirrer for 30 min at 60 °C. The silver nanowire solution was diluted to a concentration of 0.5 mg/mL using ethanol, and dispersed for 1 h by ultrasonication. Then 20, 40, 100, or 200 mL of silver nanowire solution were added to 0.1 g PSLC mixed solution, respectively, resulting in 0.01, 0.02, 0.05, 0.1 wt% of silver nanowires concentration in PSLC. After another 30 min of ultrasonication, the mixtures were placed at room temperature for 72 h to remove the ethanol.

The PSLC mixtures with different silver nanowire concentration were filled into a cell with 5 μm gap and ITO electrode on both internal surface by capillary force at 60 °C. The samples were cooled on hot stage to room temperature slowly after the cells were fully filled. Then, the samples were photo polymerized by 320–400 nm UV light with light intensity of 500 mW/cm^2 for 300 s at room temperature.

2.3. Electro-Optical Property Characterization

The alternating electric field with a square wave function was provided by a function generator (33220A, Agilent Technologies Inc., Santa Clara, CA, United States). The electric signal from the function generator was amplified through a high-voltage linear amplifier (F20A, FLC Electronics AB, Partille, Sweden). The output voltage was measured by an oscilloscope (DSOX3032T, Keysight Technologies, Santa Rosa, CA, United States). Transmittance of the samples were measured by spectrometer (HR2000+, Ocean Optics Inc., Largo, FL, United States). The wavelength of 550 nm was select to evaluate the transmittance. A halogen lamp (LS-3000, Keyence (CHINA) Co., Ltd., Shanghai, China) was used to provide white light. Response time of the samples were measure by photodiode (FSD1010, Thorlab Inc., Newtown, NJ, United States) with time resolution of 65 ns. The output signal of photodiode was amplified and then transformed by an acquisition card (USB6002, National Instruments, Austin, TX, United States), then collected by computer with a LabVIEW program. A 5 W White LED was used to provide white light. The experiment setup is shown in Figure 4.

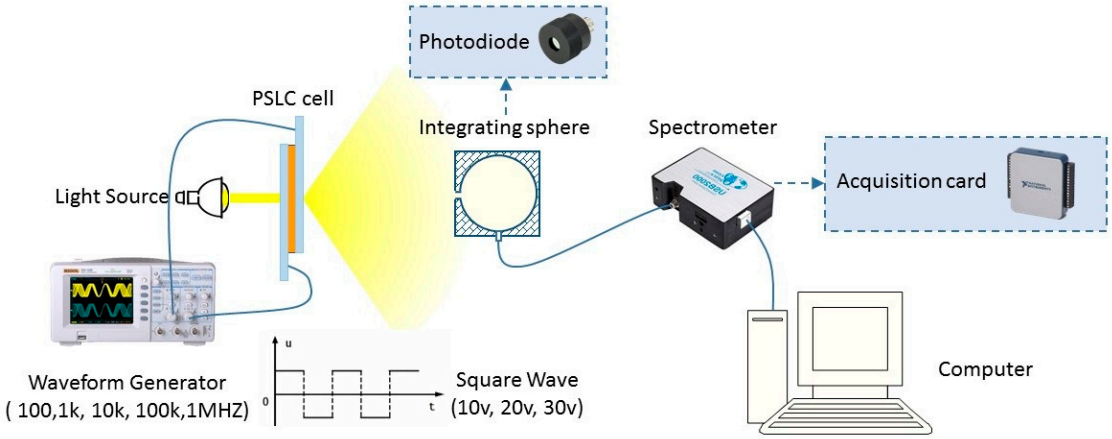

Figure 4. Experiment setup for transmittance and response time measurement (when measuring response time, the integrating sphere was replaced with a photodiode, while the spectrometer was replaced by amplifier and acquisition card).

3. Results and Discussion

3.1. Effect of Ag Nanowires on the Driving Voltage of PSLC Devices

The voltage–transmittance (V–T) curves, threshold voltages and leakage current of the Ag nanowire doped PSLC according to the Ag nanowire concentration are shown in Figure 5. The V–T curve of PSLC devices under 1 kHz square wave AC driving are shown in Figure 5a. All PSLC devices have transmittance above 95% at off state and the transmittance decreases as the voltage increases. All devices can reach a scattering state with transmittance under 18%. However, the transmittance at both on and off state decreased slightly with small amount of Ag nanowire doping at 0.01 wt.%, and the transmittance increased as the Ag nanowire concentration was increased up to 0.1 wt.%. This is because, when the concentration is too high, Ag nanowires cannot be evenly distributed in the LC and tend to aggregate together, resulting in the interconnection between the silver nanowires [34]. When the voltage continuously increased, aggregation of silver nanowires will form a local short circuit and burn up the device, thus affecting the device performance and increasing the transmittance of the device.

Meanwhile, the V–T curve of the PSLC had a different tendency: the threshold voltages (V_{10} and V_{90}) shifted as a function of the Ag nanowire concentration. It shifted to the left side first as the Ag nanowire concentration increased to 0.02 wt.%, and then shifted to the right side as the Ag nanowire concentration continued to increase. The V–T curve of PSLC devices doped with 0.01 wt.%, 0.02 wt.%, and 0.05 wt.% Ag nanowires are on the left side of the undoped PSLC device. However, the V–T curve of PSLC device doped with 0.1 wt.% Ag nanowires is on the right side of the undoped PSLC device, meaning it has worse performance than the undoped PSLC device. The voltages for 10% transmission (V_{10}) and 90% transmission (V_{90}) show the same tendency. As shown in Figure 5b, V_{10} and V_{90} greatly decreased with a small amount of doping at 0.01 wt.% Ag nanowires, and the values decreased as the Ag nanowire concentration was increased up to 0.02 wt.%. However, the V_{10} and V_{90} values started increasing when the Ag nanowire concentration continued increasing up to 0.1 wt.%. When the doping concentration is 0.02 wt.%, the threshold voltage is lowest, reduced by 35–42% compared with undoped PSLC device.

The reduction of the residual DC voltage through metal nanomaterial doping in the nematic LC is discussed in the literature [35,36]. Metal nanomaterials mixed in LC materials can capture ionic impurities and enhance the electro-optic properties of LCs. Due to the small size effect of the silver nanowire, when a voltage is applied, the surface of the silver nanowire will be polarized, and thus the ionic impurities in the liquid crystal mixture will be absorbed by the silver nanowire surface. Therefore, the reason that doping a certain concentration of Ag nanowires can reduce the threshold voltage of

the PSLC device is Ag nanowire doping can effectively eliminate the ionic impurities in the LC and reduce the conductivity in the PSLC device. Figure 5c shows the current–voltage curves of PSLC devices doped with different concentrations of Ag nanowires. At a certain voltage, the current of PSLC devices doped with 0.01 wt.% and 0.02 wt.% Ag nanowires decreasing when the concertation of Ag nanowire increases. When the Ag nanowire doping concentration is 0.02 wt.%, the current is the lowest, which represents the lowest conductivity. This is because the ionic impurities in the PSLC mixture is captured by the Ag nanowires. When the conductivity of LC material is the lowest, the electric field and force applied on the liquid crystal molecule is the strongest. Therefore, the threshold voltage is the lowest and the response is the fastest. As a result, small amount of Ag nanowire doping can reduce the amount of ionic impurities and device conductivity effectively, making the device have a better electro-optical response. This result is consistent with the V–T curves and threshold voltage variation tendency in Figure 5a,b. Since the length of the silver nanowires used in this study is about 20 μm, the density of Ag nanowire was too high when the doping concentration of the Ag nanowires increased to 0.05 wt.% and 0.1 wt.%. and the Ag nanowires became short-circuited with each other and increased the conductivity, causing the actual electric field to decrease and the driving voltage to increase.

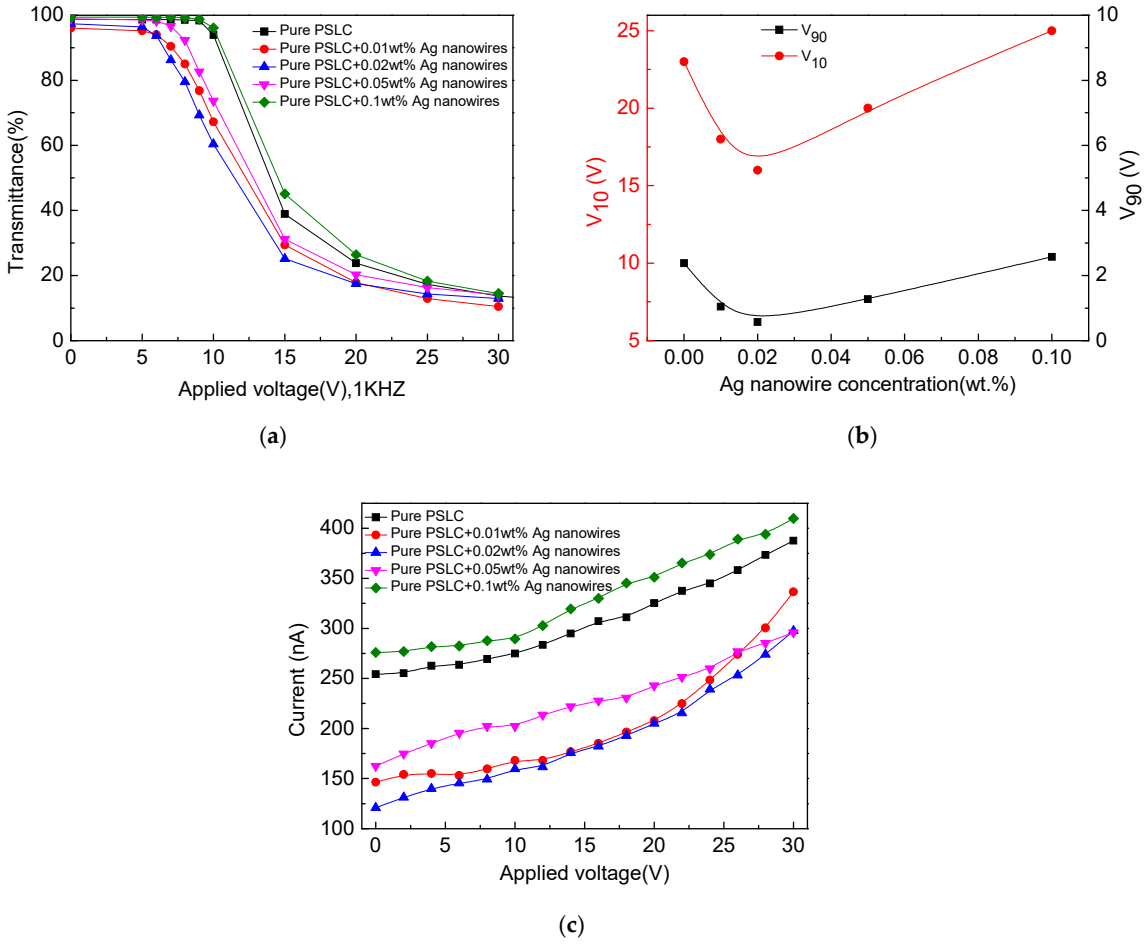

Figure 5. Voltage–Transmittance (V–T) curves, threshold voltages and leakage current of the Ag nanowire doped PSLC according to the Ag nanowire concentration: (**a**) V–T curve; (**b**) variations in voltages for 10% transmission (V_{10}) and voltages for 90% transmission (V_{90}); and (**c**) leakage current according to the Ag nanowire concentration.

3.2. Effect of Ag Nanowires on Response Time of PSLC Devices

The response time of PSLC with different Ag nanowire concentration with 30 V, 1 kHz square wave driving is shown in Figure 6a. Here, both the turn on or rising time from clear state to scattering state (an interval from 90% transmittance to 10% transmittance) and the turn off or falling time shows the same variation tendency with threshold voltage as the Ag nanowire concentration increases. The turn on time of PSLC first decreased to about a half and then increased to about double of undoped PSLC as Ag nanowire concentration increased. However, the change of turn off time was very limited, with all around 5 ms.

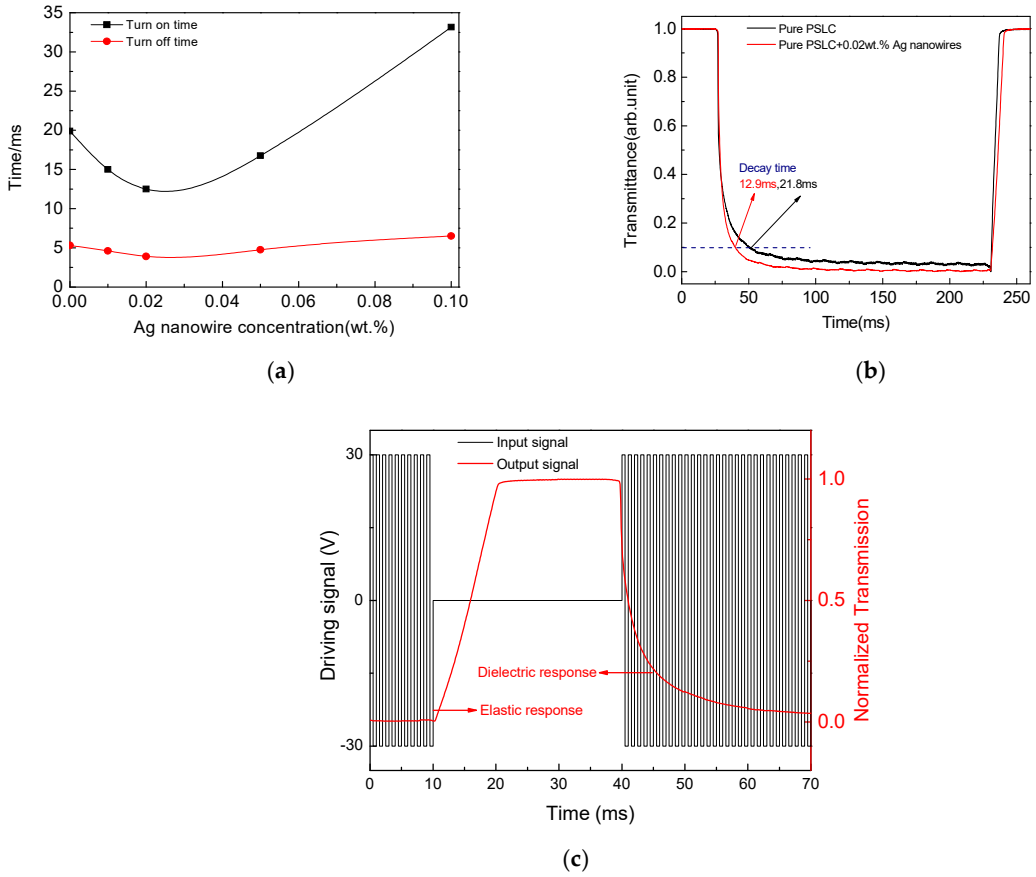

Figure 6. Response time of the Ag nanowire doped PSLC according to the Ag nanowire concentration: (**a**) response time according to the Ag nanowire concentration; (**b**) comparison of response time of pure PSLC and 0.02 wt.% Ag nanowire doped PSLC; and (**c**) input signal and output signal of PSLC with 0.02 wt.% Ag nanowire.

Figure 6b shows the comparison of temporal response of a pure PSLC and a PSLC with 0.02 wt.% Ag nanowire doping. There was no noticeable difference in the turn off time of the samples, but the turn on time of PSLC with 0.02 wt.% Ag nanowire doping was only 12.9 ms, i.e. 41% lower than the undoped PSLC.

Figure 6c shows the input signal and output signal of a PSLC with 0.02 wt.% Ag nanowire doping. It shows the Ag nanowire doped PSLC has very fast response to electric field. The turn off process of a PSLC device is elastic response, during which the negative LC molecule reorientation is driven by the vertical alignment layer and vertical aligned LC network. This process is almost linear and the Ag nanowire doping had very little influence on it. The turn on process is dielectric response. Ag nanowire doping can lower the ionic impurities in LC, which would enhance the electric field and thus increase the speed of dielectric response. On the other hand, Ag nanowire doping can increase the polar anchoring energy in the PSLC [37], which would also shorten the turn on time.

3.3. Effect of Ag Nanowires on Frequency Response of PSLC Devices

Figure 7a–c shows the transmittance versus driving frequency curve of PSLC device with different Ag nanowire doping concentration at 10 V, 20 V and 30 V respectively. At 10 V, the transmittance of all PSLC devices decreases first and then increase as the frequency increases. Lowest transmittance can be obtained at 10 kHz. At 20 V and 30 V, the change of transmittance from 100 Hz to 100 kHz is negligible. At 1 MHz, the PSLC devices stop responding to electric field, which may be because this frequency is higher than the crossover frequency (f_c) of the dielectric anisotropy of the LC used in this experiment. Under high driving voltage, the difference between PSLC devices with different Ag nanowire doping concentration is very small. The difference of F–T curves under low driving voltage is mainly caused by the variation of threshold voltage. As shown in Figure 7d, from 100 Hz to 10 kHz, the threshold voltage of all PSLC devices first decreases and then increases as the frequency increases. This trend is the same for all PSLC devices. This is because the dielectric constants of LC used in this study increase first and then decrease as a function of the frequency regardless of Ag nanowire doping concentration. The influence of driving frequency on the response time of PSLC at 30 V with different Ag nanowire doping concentration is shown in Figure 7e. It shows that, with the gradual increase in frequency, from 100 Hz to 10 kHz, the device response time has a slight downward trend, but not much. When the frequency increases from 10 kHz to 100 kHz, the response time gradually increases as the frequency increases. This trend is also the same for all PSLC devices. Therefore, the PSLC devices in this study have a good frequency modulation property, but the Ag nanowire doping has very little influence on the frequency response.

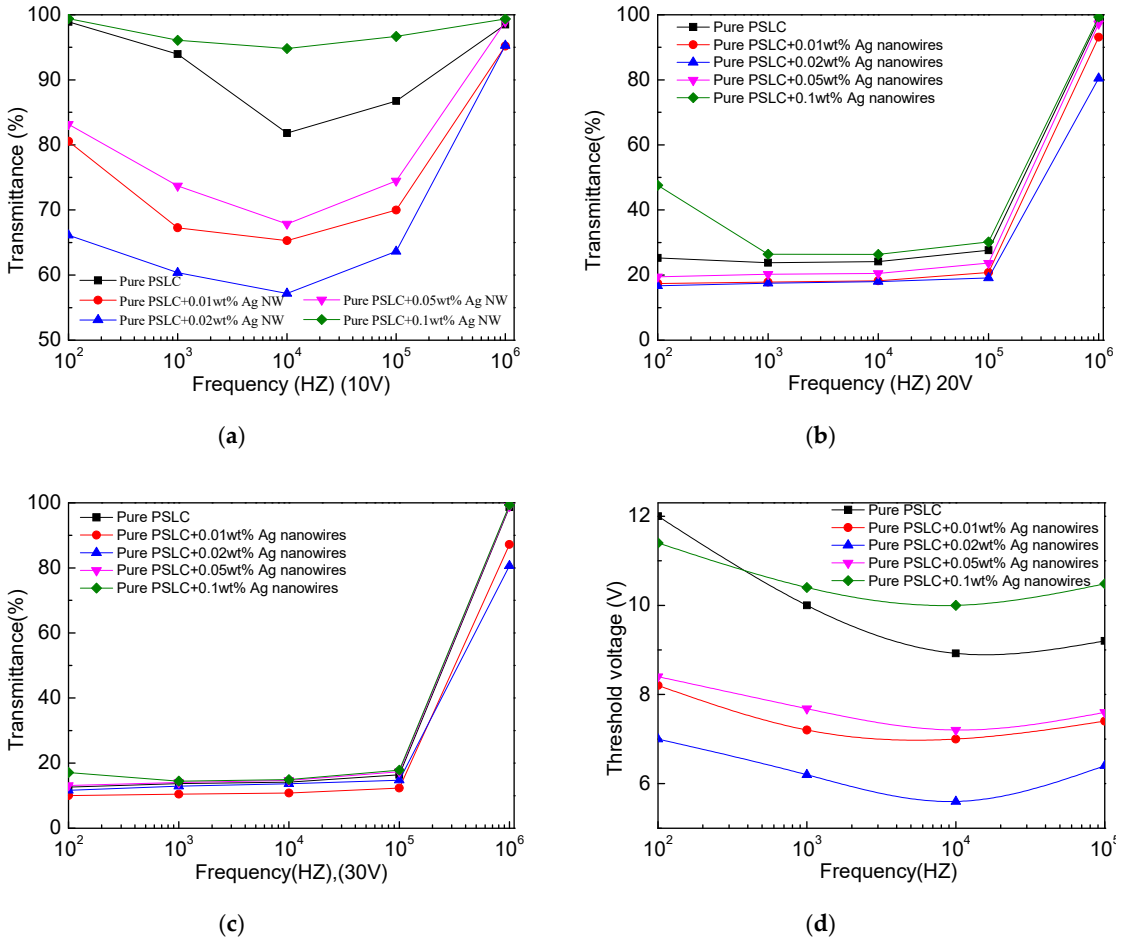

Figure 7. *Cont.*

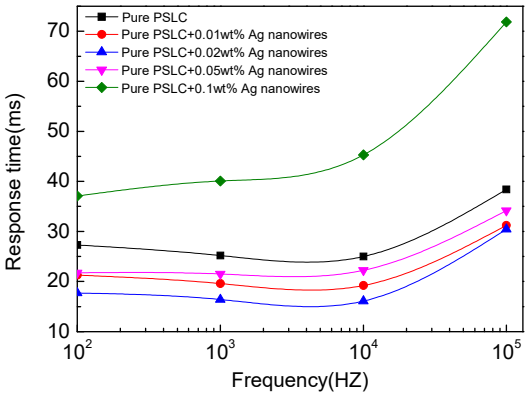

(**e**)

Figure 7. Frequency modulation of the Ag nanowire doped PSLC according to the Ag nanowire concentration: (**a**,**b**,**c**) F–T curve under 10 V, 20 V and 30 V, respectively; (**d**) threshold voltage V_{10} under different frequency; and (**e**) response time under different frequency.

4. Conclusions

Electro-optical properties of PSLC device were successfully improved by Ag nanowires doping into PSLC active layer. When doping concentration is only 0.02 wt.%, the threshold voltage V_{10} and V_{90} values can be reduced by 35–42% compared to undoped PSLC device. The main reason is Ag nanowire doping can effectively eliminate the ionic impurities in LC and thus reduce the conductivity of PSLC active layer. The turn on response time of PSLC device with 0.02 wt.% Ag nanowire doping is only 12.9 ms, which is 41% lower than that of undoped PSLC device. However, the change of turn off response time is negligible. This is because Ag nanowire doping can increase the polar anchoring energy and lower the ionic impurities in LC mixture, thus enhancing the dielectric response of LC molecules. Since the turn off process is an elastic response, doping has limited influence on this. The Ag nanowire doped PSLC shows similar frequency modulation performance with undoped PSLC device, with no significant improvement. All the present results imply that Ag nanowire doping can improve the performance of electro-optical devices such as adaptive optics devices, e.g. PSLC smart windows, which in general require a fast response and low threshold voltage.

Author Contributions: Conceptualization, X.Y. and W.L.; methodology, X.Y.; data curation, X.Y. and Y.Z.; writing—original draft preparation, X.Y. and D.Y.; writing—review and editing, W.Z. and X.H.; and supervision, D.Y. and G.Z.

Funding: This research was funded by the National Natural Science Foundation of China (Nos. 21711530647 and 51561135014), Science and technology project of Guangdong Province (Nos. 2018A050501012 and 2017B020240002), and Guangdong Innovative Research Team Program (No. 2013C102).

Acknowledgments: This work was also supported by the National Center for International Research on Green Optoelectronics, MOE International Laboratory for Optical Information Technologies, Guangdong Provincial Key Laboratory of Optical Information Materials and Technology, the 111 Project and Yunnan expert workstation (No. 2017IC011).

Conflicts of Interest: The authors declare no conflict of interest. The funders had no role in the design of the study; in the collection, analyses, or interpretation of data; in the writing of the manuscript, or in the decision to publish the results.

References

1. Baetens, R.; Jelle, B.P.; Gustavsen, A. Properties, requirements and possibilities of smart windows for dynamic daylight and solar energy control in buildings: A state-of-the-art review. *Sol. Energy Mater. Sol. Cells* **2010**, *94*, 87–105. [CrossRef]
2. Lampert, C.M. Large-area smart glass and integrated photovoltaics. *Sol. Energy Mater. Sol. Cells* **2003**, *76*, 489–499. [CrossRef]

3. Kirton, J. The physics of liquid crystals. *Opt. ACTA Int. J. Opt.* **1975**, *22*, 158. [CrossRef]
4. Bahadur, B. Liquid crystals—Applications and uses. *J. Soc. Inf. Disp.* **2012**, *2*, 63–64. [CrossRef]
5. Collings, P.J.; Hird, M. Introduction to liquid crystals: Chemistry and physics. *Am. J. Phys.* **1998**, *66*, 551. [CrossRef]
6. Deb, S.K. A novel electrophotographic system. *Appl. Optics* **1969**, *8* (Suppl. 1), 192–195. [CrossRef]
7. Macrelli, G. Optical characterization of commercial large area liquid crystal devices. *Sol. Energy Mater. Sol. Cells* **1995**, *39*, 123–131. [CrossRef]
8. Yang, D.K.; Chien, L.C.; Doane, J.W. Cholesteric liquid crystal/polymer dispersion for haze-free light shutters. *Appl. Phys. Lett.* **1992**, *60*, 3102–3104. [CrossRef]
9. Chiu, H.W.; Kyu, T. Equilibrium phase behavior of nematic mixtures. *J. Chem. Phys.* **1995**, *103*, 7471–7481. [CrossRef]
10. Dierking, I. Polymer network–stabilized liquid crystals. *Adv. Mater.* **2010**, *12*, 167–181. [CrossRef]
11. Hinojosa, A.; Sharma, S.C. Effects of gold nanoparticles on electro-optical properties of a polymer-dispersed liquid crystal. *Appl. Phys. Lett.* **2010**, *97*, 081114. [CrossRef]
12. Dierking, I. Recent developments in polymer stabilised liquid crystals. *Polym. Chem.* **2010**, *1*, 1153–1159. [CrossRef]
13. Pande, M.; Tripathi, P.K.; Misra, A.K.; Manohar, S.; Manohar, R.; Singh, S. Dielectric and electro-optical properties ofpolymer-stabilized liquid crystal system. *Appl. Phys. A* **2016**, *122*, 1–9. [CrossRef]
14. Sun, J.; Wu, S.-T. Recent advances in polymer network liquid crystal spatial light modulators. *J. Polym. Sci. Part B Polym. Phys.* **2013**, *52*, 183–192. [CrossRef]
15. Yan, J.; Rao, L.; Jiao, M.; Li, Y.; Cheng, H.-C.; Wu, S.-T. Polymer-stabilized optically isotropic liquid crystals for next-generation display and photonics applications. *J. Mater. Chem.* **2011**, *21*, 7870–7877. [CrossRef]
16. Zou, J.; Fang, J. Adhesive polymer-dispersed liquid crystal films. *J. Mater. Chem.* **2011**, *21*, 9149–9153. [CrossRef]
17. Kumar, S. Discotic liquid crystal-nanoparticle hybrid systems. *NPG Asia Mater.* **2014**, *6*, e82. [CrossRef]
18. Blanc, C.; Coursault, D.; Lacaze, E. Ordering nano- and microparticles assemblies with liquid crystals. *Liq. Cryst. Rev.* **2013**, *1*, 83–109. [CrossRef]
19. Garbovskiy, Y.; Zribi, O.; Glushchenko, A. Emerging applications of ferroelectric nanoparticles in materials technologies, biology and medicine. In *Advances in Ferroelectrics*; IntechOpen: London, UK, 2013; pp. 475–497. [CrossRef]
20. Singh, U.B.; Dhar, R.; Dabrowski, R.; Pandey, M.B. Influence of low concentration silver nanoparticles on the electrical and electro-optical parameters of nematic liquid crystals. *Liq. Cryst.* **2013**, *40*, 774–782. [CrossRef]
21. Garbovskiy, Y.; Glushchenko, I. Nano-objects and ions in liquid crystals: Ion trapping effect and related phenomena. *Crystals* **2015**, *5*, 501–533. [CrossRef]
22. Chou, T.-R.; Hsieh, J.; Chen, W.-T.; Chao, C.-Y. Influence of particle size on the ion effect of TiO_2 nanoparticle doped nematic liquid crystal cell. *Jpn. J. Appl. Phys.* **2014**, *53*, 071701. [CrossRef]
23. Haraguchi, F.; Inoue, K.I.; Toshima, N.; Kobayashi, S.; Takatoh, K. Reduction of the threshold voltages of nematic liquid crystal electrooptical devices by doping inorganic nanoparticles. *Jpn. J. Appl. Phys.* **2007**, *46*, 796–797. [CrossRef]
24. Jung, H.-Y.; Kim, H.-J.; Yang, S.; Kang, Y.-G.; Oh, B.-Y.; Park, H.-G.; Seo, D.-S. Enhanced electro-optical properties of Y2O3 (yttrium trioxide) nanoparticle-doped twisted nematic liquid crystal devices. *Liq. Cryst.* **2012**, *39*, 789–793. [CrossRef]
25. Barnes, W.L.; Dereux, A. Surface plasmon subwavelength optics. *Nature* **2003**, *424*, 824. [CrossRef] [PubMed]
26. Yaroshchuk, O.V.; Dolgov, L.O. Electro-optics and structure of polymer dispersed liquid crystals doped with nanoparticles of inorganic materials. *Opt. Mater.* **2007**, *29*, 1097–1102. [CrossRef]
27. Yaroshchuk, O.V.; Dolgov, L.O.; Kiselev, A.D. Electro-optics and structural peculiarities of liquid crystal-nanoparticle-polymer composites. *Phys. Rev. E Stat. Nonlin. Soft Matter Phys.* **2005**, *72*. [CrossRef] [PubMed]
28. Lee, J.-H.; Lee, J.J.; Lim, Y.J.; Kundu, S.; Kang, S.-W.; Lee, S.H. Enhanced contrast ratio and viewing angle of polymer-stabilized liquid crystal via refractive index matching between liquid crystal and polymer network. *Opt. Express* **2013**, *21*, 26914–206920. [CrossRef]

29. Choi, B.; Song, S.; Jeong, S.M.; Shung, S.-H.; Glushchenko, A. Electrically tunable birefringence of a polymer composite with long-range orientational ordering of liquid crystals. *Opt. Express* **2014**, *22*, 18027–18035. [CrossRef]
30. Choi, B.; Yang, K.J.; Chung, S.H. Luminance enhancement of electroluminescent devices using highly dielectric UV-curable polymer and oxide nanoparticle composite. *Opt. Mater. Express* **2014**, *4*, 1824–1832. [CrossRef]
31. Cho, Y.H.; He, M.; Kim, B.K. Improvement of holographic performance by novel photopolymer systems with siloxane-containing epoxides. *Sci. Technol. Adv. Mater.* **2004**, *5*, 319–323. [CrossRef]
32. Choi, Y.; Kim, C.S.; Jo, S. Spray deposition of Ag nanowire–graphene oxide hybrid electrodes for flexible polymer–dispersed liquid crystal displays. *Materials* **2018**, *11*, 2231. [CrossRef] [PubMed]
33. Zhang, T.; Cong, Y.; Zhang, B. Preparation and characterisation: PSCLC film doping with FexNiy nanoparticles. *Liq. Cryst.* **2015**, *42*, 167–173. [CrossRef]
34. Sannicolo, T.; Lagrange, M.; Cabos, A. Metallic nanowire-based transparent electrodes for next generation flexible devices: A review. *Small* **2016**, *12*, 6052–6075. [CrossRef] [PubMed]
35. Lee, H.M.; Chung, H.K.; Park, H.G. Residual DC voltage-free behaviour of liquid crystal system with nickel nanoparticle dispersion. *Liq. Cryst.* **2014**, *41*, 247–251. [CrossRef]
36. Yong-Seok, H.; Hyung-Jun, K.; Hong-Gyu, P. Enhancement of electro-optic properties in liquid crystal devices via titanium nanoparticle doping. *Opt. Express* **2012**, *20*, 6448–6455. [CrossRef]
37. Shin-Ying, L.; Liang-Chy, C. Carbon nanotube doped liquid crystal OCB cells: Physical and electro-optical properties. *Opt. Express* **2008**, *16*, 12777–12785. [CrossRef]